

Studies on the Intramolecular Electron Transfer Catalyzed Thermolysis of 1,2-Dioxetanes

Ana L. P. Nery,^a Dieter Weiß,^b Luiz H. Catalani^a and Wilhelm J. Baader^{a,*}

^aInstituto de Química, Universidade de São Paulo, CP 26077, 05513-970, São Paulo, Brazil

^bInstitut für Organische und Makromolekulare Chemie, Friedrich-Schiller-Universität Jena, Humboldtstr. 10, D-07743 Jena, Germany

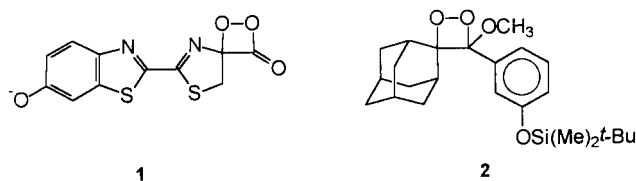
Received 23 February 2000; accepted 26 May 2000

Abstract—This work reports the synthesis and the chemiluminescence properties of the dioxetanes: 4-ethyl-4-methyl-3-(3-methoxyphenyl)-1,2-dioxetane (**I**), 4-ethyl-4-methyl-3-(3-*tert*-butyldimethylsilyloxyphenyl)-1,2-dioxetane (**II**), 4,4-dimethyl-3-(3-methoxybenzyl)-1,2-dioxetane (**III**) and 4,4-dimethyl-3-(3-*tert*-butyldimethylsilyloxybenzyl)-1,2-dioxetane (**IV**). While in the thermal decomposition of **I–IV** preferential formation of triplet excited states is observed, in the presence of fluoride ions the decomposition rate constants of **II** and **IV** increase drastically and singlet excited states are formed with high quantum yields. These results are discussed based on the CIEEL ('Chemically Initiated Electron Exchange Luminescence') mechanism where the decomposition of the dioxetanes should be initiated by an intramolecular electron transfer from the phenolate ion (generated by fluoride catalyzed deprotection of the silyloxy group), either directly bound to the peroxidic ring (**II**) or separated from it by a methylene bridge (**IV**). © 2000 Elsevier Science Ltd. All rights reserved.

Introduction

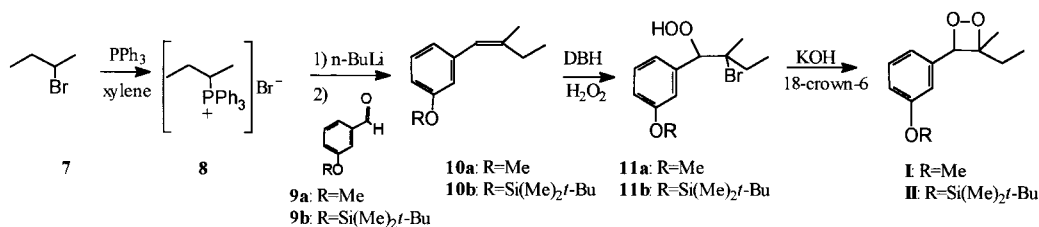
The phenomenon of luminescence generated either by living organisms (bioluminescence) or by chemical processes (chemiluminescence) has become an important analytical tool in recent years, in particular for biomedical applications. The chemiluminescent reaction most investigated over the past 30 years is the decomposition of 1,2-dioxetanes.¹ Well before these were first prepared and isolated by Kopecky and Mumford in 1969,² 1,2-dioxetanes were proposed as key intermediates in several chemi- and bioluminescent reactions.³ The thermal cleavage of 1,2-dioxetanes generates two carbonyl fragments, one of which can be formed in an electronically excited state, predominantly in the triplet state.^{1,4–6} However, when these high-energy molecules bear an electron-rich substituent, singlet states are obtained predominantly.⁵ In these cases, such dioxetanes become labile and display 'chemically initiated electron exchange luminescence' (CIEEL), an electron transfer mechanism originally proposed by Schuster for the decomposition of diphenylperoxide^{7,8} and latter for α -peroxylactones^{9,10} and various other peroxides.^{11–15} The electron transfer may proceed either inter- or intramolecularly. An efficient intramolecular CIEEL is considered to take place in the firefly bioluminescence, where an α -peroxylactone (**1**) was proposed as intermediate.¹⁶ 1,2-Dioxetanes containing substituents with low oxidation potentials,⁵ such as aryl-O⁻, aryl-RN⁻ function-

alities, display intramolecular CIEEL. The most successful design of an intramolecular CIEEL system is based on spiroadamantane-substituted dioxetanes with a protected phenolate ion (**2**).^{17–19} The advantage of such dioxetanes is their thermal persistence and their convenient synthesis through photooxygenation. The decomposition of these dioxetanes can be achieved on treatment with an appropriate reagent (trigger) to induce phenolate ion release. These phenolate-initiated intramolecular CIEEL processes provide the basis for numerous commercial applications, most prominently in chemiluminescence immunoassays.^{20–23} Thus, the search for other triggerable CIEEL-active dioxetanes goes on attracting the interest of many research groups;²⁴ however, with only a few exceptions,^{25–28} the efficiency of the light emission from these systems is often very low.^{29,30}



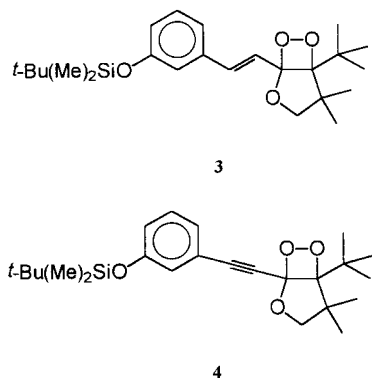
Most of the recent work in this field has been devoted to the synthesis of stable dioxetanes with triggering functionalities, in the search for efficient chemiluminescent systems useful in analytical applications. Recently, Matsumoto et al.²⁶ have described the synthesis of dioxetanes containing a phenylethyl group (**3**) or a phenylethynyl group (**4**) as substituent, whose fluoride-catalyzed decomposition in

Keywords: 1,2-dioxetanes; electron transfer; chemiluminescence; CIEEL.
* Corresponding author. Tel.: +49-5511-38183814; fax: +49-5511-38155579; e-mail: wjbaader@iq.usp.br



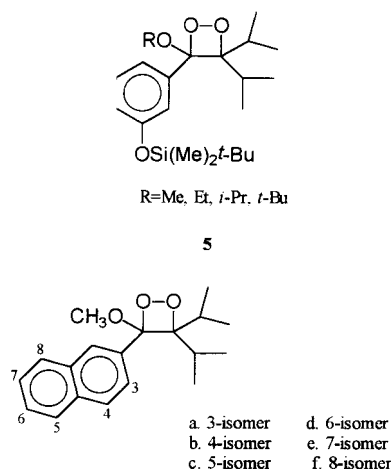
Scheme 1. DBH: 1,3-dibromo-5,5-dimethylhydantoin.

DMSO yields red light with relatively high quantum yields.



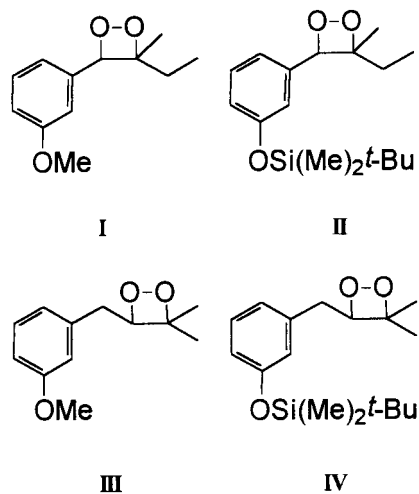
Other work describes the synthesis and thermal decomposition of 1-alkoxy-1-aryl-2,2-diisopropylethylenes substituted dioxetanes (**5**), whose fluoride catalyzed decomposition leads to an intense blue light with chemiluminescence quantum yields higher than 0.2.²⁷

However, although CIEEL remains a controversial proposition, mechanistic studies devoted to its features are rare. The decomposition mechanism of these dioxetanes has not yet been totally clarified, especially when the electron transfer occurs intramolecularly and these reactions are very fast. Recent discussions were directed to the odd/even relationship for the catalyzed decomposition of 3,3-diisopropyl-4-methoxy-4-(siloxy-2-naphthyl)-1,2-dioxetanes (**6**)²⁸ and to the solvent-cage effect on the decomposition of dioxetane **2**.³¹ In the latter case, the authors propose that the back electron transfer process is the key step in chemiexcitation.



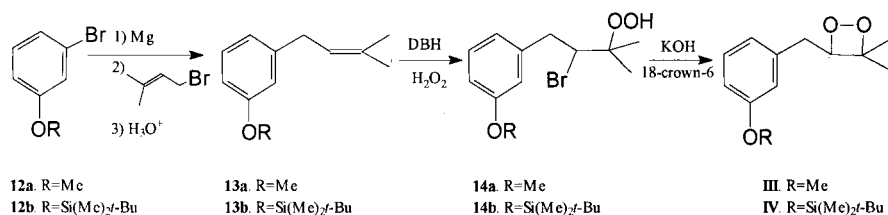
In a previous communication,³² we report some of the chemiluminescence characteristics of dioxetanes **II** and **IV** upon unimolecular and fluoride catalyzed decomposition. In this work we report the synthesis and chemiluminescent properties of the 1,2-dioxetanes **I** to **IV**. Our studies include the determination of the activation parameters and quantum yields in the unimolecular decomposition of **I–IV** and of the fluoride-initiated decomposition of **II** and **IV**. Dioxetanes **I** and **III** were prepared to compare simple substituent effects on the thermolysis of 1,2-dioxetanes, thus a methoxy- or a siloxy-substituent may exert similar effects on the decomposition of the peroxidic ring.

Compounds **II** and **IV** were treated with fluoride to generate the corresponding phenolate ion either directly bound to the peroxide ring (**II**) or separated from it by a methylene bridge (**IV**), in order to verify the occurrence of an intramolecular CIEEL mechanism. In this respect, the distinction between a ‘resonance’ (**II**) and a ‘through σ -bond’ (**IV**) electron transfer from the generated phenolate to the dioxetane moiety appeared of special interest to us, due to the fact that there is no example in the literature of an intramolecular CIEEL when the electron donor and the peroxide ring are separated. Our studies indicate that an intramolecular CIEEL occurs in both cases (**II** and **IV**) in the presence of fluoride, leading to the preferential formation of singlet excited states.



Results

Dioxetanes **I** to **IV** were prepared from the corresponding olefins by the Kopecky route.² Dioxetanes **I** and **II** were obtained through a four step sequence (Scheme 1) in



Scheme 2.

approximately 10% yield as a mixture of the isomers *Z* and *E*, which were not separated. The compounds **III** and **IV** were obtained in lower yields, 1.0 and 0.1%, respectively (Scheme 2), probably due to the elimination of HBr in the reaction between the β -bromohydroperoxide and the base, generating the corresponding allylic hydroperoxide; a peroxidic compound was indeed detected as the major product of this reaction.

The dioxetanes were purified by low temperature (-35°C) silica gel chromatography column and unequivocally characterized on the basis of their spectral data (^1H and ^{13}C NMR) and decomposition products. The purity of the compounds **I** to **IV**, determined by ^1H NMR, was greater than 95% in all cases, with the decomposition products being the only detectable impurities. Furthermore, it should be pointed out that the dioxetanes **III** and **IV** do not contain traces of **I** and **II**, respectively, as the synthetic routes for obtaining them are totally different (Schemes 1 and 2). A minor product derived from the allylic 1,3-substitution

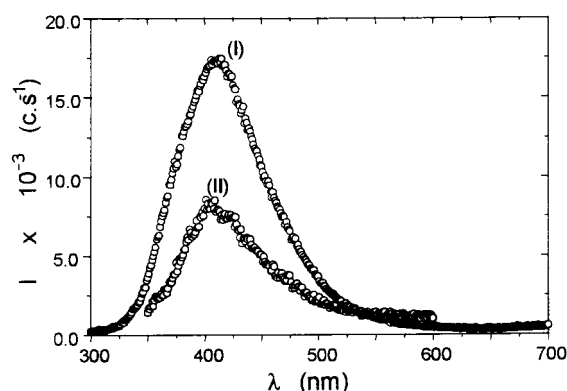


Figure 1. Spectra of the direct emission in the thermolysis of dioxetanes **I** and **II** at 80°C in toluene (**I**)= $(6.7\pm 0.8)\times 10^{-5}$ M, (**II**)= $(4.7\pm 1.0)\times 10^{-5}$ M), emission intensities (*I*) in counts s^{-1} .

($\text{S}_{\text{N}}2'$) has been observed under certain experimental conditions. However, even when these monosubstituted olefins (3-methyl-3-(3-*R*-phenyl)-1-butene, **16a**—*R*= OCH_3 , **16b**—*R*= $\text{OSi}(\text{Me})_2t\text{-Bu}$) were present as side products in the Grignard coupling reaction, the corresponding monosubstituted dioxetanes **V** and **VI** (3-(2-(3-*R*-phenyl)-isopropyl)-1,2-dioxetane, **V**—*R*= OCH_3 , **VI**—*R*= $\text{OSi}(\text{Me})_2t\text{-Bu}$) could not be detected even in traces, in the preparations of **III** and **IV**, respectively, presumably due to the highly unstable nature of monosubstituted dioxetanes.³³

Thermal decomposition of **I** to **IV** in toluene leads exclusively to the formation of the expected carbonyl cleavage products, as verified by NMR spectroscopy. Direct emission with a maximum at 412 nm is observed for **I** and **II** (Fig. 1), which should correspond to the emission of the singlet excited aromatic aldehydes as their singlet energies are lower than those of aliphatic ketones.³⁴ In the case of **III** and **IV** excited state formation can only be detected in the presence of sensitizers: 9,10-dibromoanthracene (DBA) and 9,10-diphenylanthracene (DPA).

For dioxetanes **I** and **II** the activation parameters were obtained from the temperature dependence of the decomposition rate constants by direct emission measurements, whereas for **III** and **IV** by sensitized emission (Table 1). The chemiluminescence activation parameters $\Delta H_{\text{chl}}^{\ddagger}$ were obtained by plotting the log of initial emission intensities as a function of $1/T$ instead of the rate constants in the Eyring plots.³⁵ The chemiexcitation quantum yields were obtained by utilization of the sensitizers DPA for singlet and DBA for triplet state counting,³⁶ using luminol as light standard.^{37,38} The emission profiles of dioxetane decomposition were measured at 80°C at different concentrations of DPA and DBA in toluene. The rate constants obtained for **I** to **IV** at this temperature were in the range of 3.0×10^{-3} to $4.3\times 10^{-3} \text{ s}^{-1}$ (see Experimental). The initial emission intensity (I_0) was determined for each sensitizer concentration

Table 1. Activation parameters and quantum yields for the unimolecular decomposition of dioxetanes **I–IV**

Dioxetane	$\Delta H^{\ddagger a}$	$\Delta S^{\ddagger b}$	$\Delta G^{\ddagger a}$ (25°C)	$\Delta H_{\text{chl}}^{\ddagger a}$	$\Phi^{\text{T}} (\times 10^2)$	$\Phi^{\text{S}} (\times 10^3)$	$\Phi^{\text{T}}/\Phi^{\text{S}}$
I ^c	23.6 ± 0.4	-3.8 ± 0.10	24.7 ± 0.6	22.2 ± 0.3	5.2 ± 0.8	2.3 ± 0.06	23
II ^c	24.9 ± 0.6	-0.54 ± 0.02	25.1 ± 0.6	21.3 ± 0.4	6.8 ± 1.8	3.6 ± 0.10	19
III ^d	22.6 ± 0.2	-6.1 ± 0.1	24.4 ± 0.2	26.2 ± 0.4	4.5 ± 0.8	0.16 ± 0.002	280
IV ^d	22.6 ± 0.9	-5.8 ± 0.7	24.1 ± 1.1	24.5 ± 1.0	6.6 ± 0.6	0.22 ± 0.009	307

^a In kcal mol^{-1} .

^b In $\text{cal mol}^{-1} \text{ K}^{-1}$.

^c **I**)= $(6.7\pm 0.8)\times 10^{-5}$ M, (**II**)= $(1.0\pm 0.2)\times 10^{-4}$ M, 412 nm.

^d **III**)= $(8.3\pm 0.33)\times 10^{-5}$ M, (**IV**)= $(2.1\pm 0.4)\times 10^{-5}$ M, DPA 10 mM, 438 nm.

For quantum yield determinations: **I**)= $(6.0\pm 0.7)\times 10^{-6}$ M, (**II**)= $(4.7\pm 1.0)\times 10^{-5}$ M, (**III**)= $(8.3\pm 0.3)\times 10^{-5}$ M, (**IV**)= $(2.1\pm 0.4)\times 10^{-5}$ M, 80°C , [DPA] and [DBA] from 1.7×10^{-3} to 1.0×10^{-2} M, Φ^{T} and Φ^{S} in E mol^{-1} . All data were obtained in toluene.

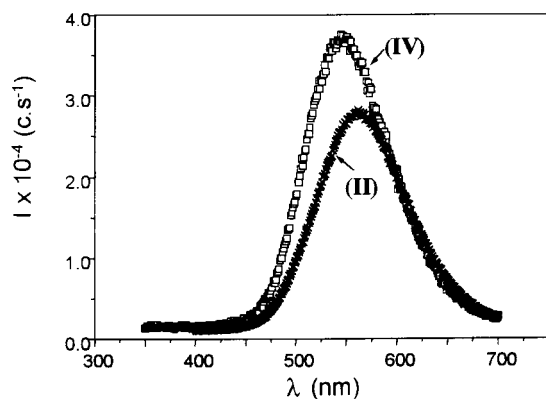


Figure 2. Direct emission spectrum for the fluoride catalyzed decomposition of dioxetanes **II** and **IV** in THF ($[F^-]=3.2\times 10^{-2}$ M, $[II]=(2.0\pm 0.4)\times 10^{-5}$ M at 25°C, $[IV]=(4.2\pm 0.8)\times 10^{-5}$ M at 7.5°C), emission intensities (I) in counts s^{-1} .

and the emission intensity at infinite sensitizer concentration obtained by extrapolation of the double-reciprocal plot $1/I_0$ versus $1/[sensitizer]$. Singlet and triplet quantum yields were calculated according to literature procedures (see Discussion).⁵

The treatment of **II** and **IV** with tetrabutylammonium fluoride (TBAF, 1.0 M solution in THF), causes deprotection of the silyloxy-substituted phenyl moiety, generating the corresponding phenolates. As a consequence, the decomposition rates increase drastically and a yellow flash of light is observed. The fluoride-initiated reactions are about 10^4 times faster than the unimolecular ones and in both cases a strong direct emission with a maximum around 550 nm is observed (Fig. 2).

At low fluoride concentrations the observed rate constants (k_{obs}) show a linear dependence on the fluoride concentration ($[F^-]$), indicating the deprotection as the rate limiting

step. However, at high fluoride concentrations, the k_{obs} values are independent of its concentration. Therefore, under these conditions k_{obs} should correspond to the decomposition of the phenolate substituted dioxetane (Fig. 3).

The activation parameters for the initiated decomposition were determined by monitoring the direct light emission of the dioxetanes in the presence of fluoride at temperatures varying from 0 to 25°C, under identical reaction conditions. For the initiated decomposition of **II**, the activation parameters were obtained at three different fluoride concentrations: 1.3×10^{-3} , 1.3×10^{-2} and 3.2×10^{-2} M, in order to verify if a variation of the fluoride concentration would exert any effect on the activation parameters. The activation enthalpies (ΔH^\ddagger) obtained at the saturation region of Fig. 3 ($[F^-]=1.3\times 10^{-2}$ and 3.2×10^{-2} M) are practically the same, while at lower fluoride concentration the ΔH^\ddagger are a little higher (ca. 1 kcal) (Table 2).

In contrast to the unimolecular decomposition, a strong, easily visible yellow emission is observed in the presence of fluoride. Due to the longer wavelength emission (Fig. 2), it was not possible in this case to use DPA and DBA for the determination of the chemiexcitation yields. No significant enhancement of the emission intensity was observed with rubrene. Thus, the singlet quantum yields were determined by measurements of the direct chemiluminescence. The chemiluminescence quantum yields (Φ_{CL}) were obtained from the integral of the emission curves, using luminol³⁷ as standard with correction for the photomultiplier sensibility (Table 2). Singlet excitation yields can be obtained from Φ_{CL} values, if the fluorescence quantum yields of the emitting species are known. As the chemiluminescence spectra of **II** and **IV** (Fig. 2) match the fluorescence spectra of the respective substituted phenolate, the decomposition products, the aromatic aldehydes appear to be the emitting species. The fluorescence quantum yields of the emitting species were determined using standard procedures³⁹ by

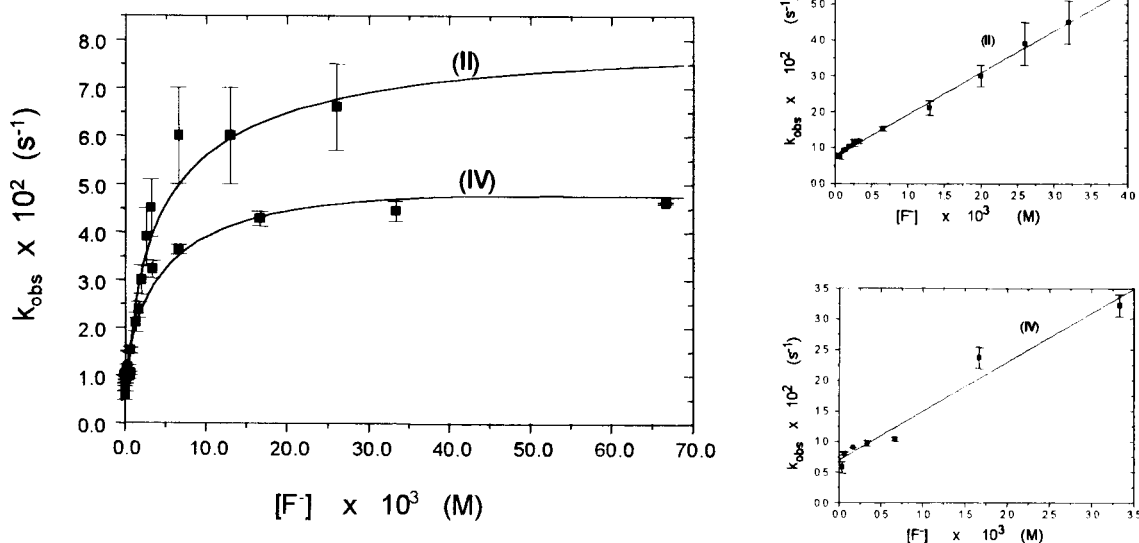


Figure 3. Dependence of the observed rate constant (k_{obs}) on $[F^-]$ for the decomposition of **II** and **IV** in THF at 25°C ($[II]=(2.0\pm 0.4)\times 10^{-5}$ M, $[IV]=(4.1\pm 0.8)\times 10^{-5}$ M).

Table 2. Activation parameters and quantum yields for the fluoride initiated decomposition of **II** and **IV**.

ΔH^\ddagger , $\Delta H_{\text{chl}}^\ddagger$ and ΔG^\ddagger in kcal mol⁻¹; ΔS^\ddagger in cal mol⁻¹ K⁻¹, [F⁻]=3.2×10⁻² M, [**II**] = (2.0 ± 0.4) × 10⁻⁵ M, λ = 560 nm, [**IV**] = (4.2 ± 0.8) × 10⁻⁵ M, THF, λ=mirror position, T: 0–25°C, for calculation of Φ^S , Φ_{FL} of the emitting species of **II** and **IV**, 0.036 and 0.0073, respectively, were obtained under the same conditions at 25°C. Data obtained in THF

Dioxetane	ΔH^\ddagger	ΔS^\ddagger	ΔG^\ddagger (25°C)	$\Delta H_{\text{chl}}^\ddagger$	Φ_{CHL} (×10 ²)	Φ^S (×10 ²)
II	20.6±0.2	5.0±0.1	19.1±0.2	16.2±0.4	3.7±0.8	100±30
IV	17.6±0.8	-5.9±0.4	19.4±1.0	19.3±1.3	0.0074±0.0018	1.0±0.3

reacting the silyloxy-substituted carbonyl compound with TBAF under the experimental conditions used for the kinetics measurements (Scheme 3). Fluorescein was chosen as standard as it shows an emission spectrum with maximum around 560 nm and its fluorescence quantum yield (ϕ_{FL}) is well established (ϕ_{FL} =0.91 in 0.1 M NaOH).³⁹

Table 2 shows that excited singlet state formation in the initiated decomposition of **II** is quantitative, although there is a large uncertainty attached to this value, due to the error progression from the original experimental data ([dioxetane] determination, photomultiplier calibration, Φ_{FL} determination). In spite of the fact that Φ^S for **IV** is two orders of magnitude lower, this yield is still very high when compared to values obtained for most intramolecular CIEEL systems.²⁹

Finally, control experiments were performed to prove the intramolecular nature of the catalysis in the decomposition of **II** and **IV**. For this purpose, the methoxy-substituted 1,2-dioxetanes **I** ([**I**]=0.7×10⁻³ M) and **III** ([**III**]=1.0×10⁻³ M) were treated with TBAF ([TBAF]=0.10 M) in the absence and the presence of the protected aldehydes **9b** and **15** (**9b**) and [**15**]=1.0×10⁻² M), respectively, in THF at 25 and 60°C. At 25°C, no measurable light emission could be observed under any experimental condition. At 60°C, the unimolecular decomposition of the dioxetanes can be observed by the direct emission of **I** and the DPA sensitized emission of **III**. The observed rate constants are not modified by the addition of TBAF or aldehydes **9b** and **15**, as well as the addition of both.

Discussion

Upon unimolecular decomposition of **I** and **II** direct emission at around 412 nm was observed, whereas for **III** and **IV** it was necessary to use sensitizers (DBA and DPA) for detecting the electronically excited state products. Compounds **I** to **IV** show typical characteristics of simple trisubstituted 1,2-dioxetanes; they are relatively stable ($\Delta G^\ddagger \cong 25$ kcal/mol) and show preferential formation of triplet excited species (Table 1). The fact that **I** and **II** were obtained as a mixture of *Z* and *E* isomers does not invalidate the discussion on the activation parameters and quantum yields, as it is known that the activation energy (E_a) and the Φ^T and Φ^S for a series of *Z/E* isomers are practically the same within the experimental error.^{33,40,41} The ratio Φ^T/Φ^S for **I** and **II**, 23 and 19, respectively, are lower than those normally observed for this kind of dioxetanes. Since no experiment was performed to determine the value for the efficiency of the triplet–singlet energy transfer (Φ^{T-S}) from the specific excited carbonyl products to DBA, Φ^{TS} was taken as 0.2.³⁶ Φ^T may be underestimated if

$\Phi^{\text{TS}} < 0.2$, as it would be if the triplet excited state energy of the carbonyl cleavage products are lower than the T₂ of DBA. On the other hand, as the absolute values for triplet quantum yields of **I** to **IV** are very similar, the obtained ratios for **I** and **II** could simply be an intrinsic characteristic of these dioxetanes, due to the higher singlet quantum yields.

The comparison of the values for the pairs **I/II** and **III/IV** shows the similarity in the thermal stability of silyloxy and methoxy substituted derivatives. The values of $\Delta H_{\text{chl}}^\ddagger$, lower than those determined by isothermal kinetics (ΔH^\ddagger) for **I** and **II**, can be attributed to a negative activation energy of the fluorescence from the excited products.³⁵ The results obtained upon unimolecular decomposition of **I** to **IV** clearly demonstrate that these compounds show chemiluminescence characteristics expected for simple trisubstituted 1,2-dioxetanes and no differences are observed for the methoxy and silyloxy substituted derivatives.

In contrast to the unimolecular decomposition, where a weak and continuous emission over about 30 min is observed at 80°C in THF, in the presence of fluoride, at 25°C, the complete decomposition of **II** and **IV** occurs in a few seconds, accompanied by an intense flash of yellow light. The half-lives at 25°C for **II** and **IV** in the absence of fluoride, 81 and 24 h, respectively, are reduced to 11 and 16 s, respectively, in the presence of the trigger. The activation parameters obtained for fluoride initiated decomposition are considerably lower than for the unimolecular one (Table 3). Moreover, the chemiluminescence spectra of the catalyzed reactions match the fluorescence spectra of the corresponding phenolates. In both cases, the decomposition profiles show first order decay and the observed rate constants (k_{obs}) are independent of the fluoride concentrations for [F⁻] > 2.0×10⁻² M, showing a linear dependence for [F⁻] < 5×10⁻³ M. These facts indicate that at lower fluoride concentrations, the decomposition rates are determined by the bimolecular reaction between the dioxetane and fluoride. As the deprotection reaction becomes faster with increasing fluoride concentration, the rate limiting step becomes the electron transfer from the generated phenolate moiety to the peroxidic ring.

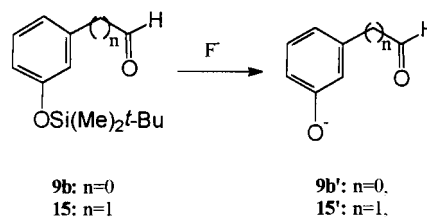
**Scheme 3.**

Table 3. Unimolecular and fluoride initiated decomposition of dioxetanes **II** and **IV**

Dioxetane	ΔH^\ddagger^a	ΔS^\ddagger^a	ΔG^\ddagger^a (25°C)	$t_{1/2}$ (25°C)	Φ^T^d ($\times 10^2$)	Φ^S^d ($\times 10^2$)
II ^b	24.9±0.7	-0.54±0.02	25.1±0.6	2.9×10 ⁵ s; 81 h	6.8±1.8	0.36±0.10
II +F ^{-c}	20.6±0.2	5.0±0.07	19.2±0.2	11 s	–	100±30
IV ^b	22.6±0.9	-5.8±0.1	24.1±1.1	8.7×10 ⁴ s; 24 h	6.6±0.6	0.022±0.01
IV +F ^{-c}	17.6±0.8	-5.9±0.4	19.4±1.0	16 s	–	1.0±0.3

^a ΔH^\ddagger and ΔG^\ddagger in kcal mol⁻¹; ΔS^\ddagger in cal mol⁻¹ K⁻¹.

^b $[\text{II}]=(1.0\pm 0.2)\times 10^{-4}$ M, $[\text{IV}]=(2.1\pm 0.4)\times 10^{-5}$ M, toluene, 65–85°C.

^c $[\text{II}]=(2.0\pm 0.4)\times 10^{-5}$ M—560 nm, $[\text{IV}]=(4.2\pm 0.8)\times 10^{-5}$ M— λ =total emission, THF, $[\text{F}]=3.2\times 10^{-2}$ M, 0–25°C.

^d Φ^T and Φ^S in E mol⁻¹.

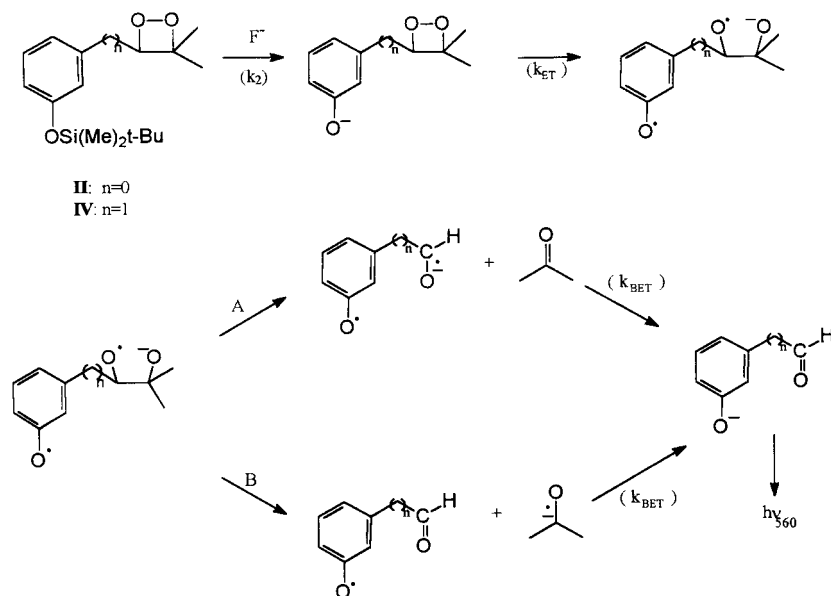
The activation parameters determined for this step for **II** and **IV** (Table 2) are reasonably similar and the ΔG^\ddagger values obtained at 25°C are identical, within the experimental error. The negative value for ΔS^\ddagger of **IV**, which compensates the surprisingly low value of ΔH^\ddagger , may be due to the need of a specific conformation for the electron transfer from the phenolate to the dioxetane ring through the methylene bridge.⁴² The ΔH^\ddagger and $\Delta H_{\text{chl}}^\ddagger$ values for dioxetane **IV** are similar and indicate that there is no major contribution of a dark decomposition pathway. The fact that the $\Delta H_{\text{chl}}^\ddagger$ is lower than the ΔH^\ddagger for **II** should be caused by the negative activation energy of the phenolate fluorescence, in analogy to the observations made in the unimolecular decomposition of **I** and **II**. In a general way, the activation parameters obtained for **II** and **IV** show that the initial electron transfer from the phenolate to the dioxetane ring occurs with the same efficiency whether the electron donor is directly linked to the acceptor ('resonance electron transfer') or connected to it by a methylene bridge ('through σ -bond electron-transfer').

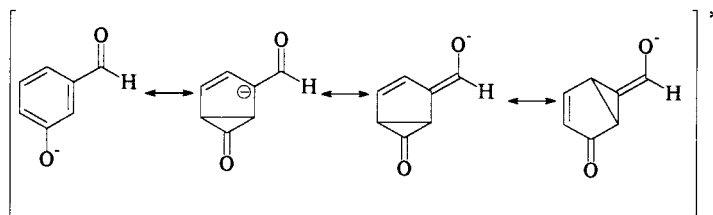
Based on the above outlined facts, we have proposed a mechanism which is consistent with the CIEEL sequence. In the first step, the generation of the free phenolate occurs, which acts as an internal electron donor to the dioxetane moiety. Following this intramolecular electron transfer, the breakdown of the peroxidic ring generates two carbonyl fragments. In the last step, the formal back electron transfer

is responsible for the generation of electronically excited states (Scheme 4).

Although the quantum yields in the initiated decomposition of **II** and **IV**, 100 and 1.0%, respectively, are very different, their magnitude is in agreement with occurrence of an intramolecular CIEEL mechanism in both cases. Control experiments using **I** and **III** in the presence of phenolates clearly exclude an intermolecular catalysis in the initiated dioxetane decomposition. Furthermore, the purity of **IV** and the fact that it cannot contain any traces of **II** (see Results) exclude the possibility that the observed emission in the initiated decomposition of **IV** might be due to impurities. It must be stated here again that the observed Φ^S for **IV**, although two orders of magnitude lower than for **II**, is still a reasonably high quantum yield if compared to intermolecular^{7–10,43} and some intramolecular CIEEL systems.^{29,30} The observed difference of two orders of magnitude of Φ^S for **II** and **IV** should be related to the efficiency of the excited state formation in the back electron transfer step (k_{BET}). In the case of **II**, the carbonyl radical anion, generated after the peroxide cleavage, represents an excited state. This hypothesis is supported by the so-called *meta*-effect, which predicts that the excited species generated in the case of **II** can be stabilized by 'resonance structures' (Scheme 5).^{44–46}

In the case of **IV** this stabilization is not possible and,

**Scheme 4.**



Scheme 5.

therefore, excited state formation by back electron transfer becomes less efficient. Moreover, in this case two pathways are possible: A and B in Scheme 4. In route A, an anion-radical derived from a non-conjugated carbonyl fragment would be formed. Although in this case the back electron transfer would be intramolecular too, it should be less efficient for excited state generation than for **II**, due to the impossibility of electronic conjugation between the electron donor and electron receptor species. In route B, an anion-radical derived from acetone could be formed, which means that the back electron transfer, responsible for generation of the excited states would proceed intermolecularly, resulting in reduced quantum yields. Escape from the solvent cage would cause a decrease in the singlet chemiexcitation yield, as previously described for the catalyzed decomposition of a spiroadamantyl-substituted dioxetane.³¹

In summary, the fluoride initiated decomposition of **IV** constitutes the first example of an intramolecular CIEEL mechanism, initiated by electron transfer from a donor which is not directly bound or conjugated to the peroxide ring. A comparison of the results obtained with **II** and **IV** shows that the initial electron transfer occurs with similar efficiency whether the donor is directly linked to the dioxetane ring or separated by a methylene bridge, indicating that efficient electron transfer can occur through the σ -bond.⁴² The intramolecular nature of this electron transfer has been unequivocally demonstrated by control experiments with the methoxy-substituted dioxetanes **I** and **III** in the presence of external phenolate ions. Two alternative interpretations are given for the much lower singlet quantum yields in the initiated decomposition of **IV** as compared to **II**. Whereas the reaction sequence is completely intramolecular for **II** and the excited state of the aromatic cleavage product is formed directly, in agreement with the unit singlet quantum yield ($\Phi^S=1.0 \text{ E mol}^{-1}$), the back-electron transfer for **IV** can be an intramolecular (Scheme 4, route A) or an intermolecular (Scheme 4, route B) process. The lower Φ^S for **IV** is caused by the lack of conjugation of the carbonyl anion radical with the aromatic ring in the intramolecular back-electron transfer, showing that in this case the methylene group considerably slows down the electron transfer process (or the electron transfer leads mainly to formation of the ground state product). In the intermolecular back-electron transfer, radical ion pair escape from the solvent cage may considerably lower Φ^S .

This mechanistic model adequately explains the chemiluminescence parameters and the quantum yields obtained in the initiated decomposition of **II** and **IV** and therefore supplies additional evidence for the validity of the intramolecular CIEEL mechanism. However, this model is not in full

agreement with the conclusions of a study on the viscosity dependence of the quantum yields obtained in the initiated decomposition of a spiroadamantyl-substituted dioxetane, where an intermolecular back-electron transfer is proposed in the excitation step.³¹ Nevertheless, this latter mechanism cannot account for the high Φ^S generally obtained in the intramolecular initiated dioxetane decomposition,^{18,19,25–28,32} as compared to the inefficient intermolecular CIEEL systems.^{7–10,43} These discrepancies clearly demonstrate that more mechanistic studies, using different model compounds, are necessary.

Experimental

Solvents and commercially available reagents were purified by usual procedures.⁴⁷ Tetrahydrofuran and diethylether were freshly distilled from sodium and benzophenone under nitrogen. The dichloromethane and hexane, used for chromatographic purification of the dioxetanes were dried over CaH_2 , distilled, left overnight over EDTA, filtered and distilled again.

The formation of products and consumption of reagents were followed on a Shimadzu CG14A gas chromatography coupled to a flame ionization detector, using a megabore column CBP1W25 100 (id: 0.53 mm, film thickness; 1.0 μm , L : 25 m). The ^1H and ^{13}C NMR spectra were obtained in CDCl_3 on a Bruker AC-200F and the mass spectrum on a CG-MS Hewlett-Packard: 5890 (Chromatography) and 5988 (mass).

Dioxetanes I–IV

2-Butyltriphenylphosphoniumbromide (8).⁴⁸ 2-bromobutane (**7**, 0.05 mol) and triphenylphosphine (0.05 mol), in 20 mL anhydrous xylene were heated in a sealed flask for 90 h at 160°C. The white crystals obtained were washed with cold xylene and dried under vacuum for 4 h (100°C/2 mmHg), yielding 80% of product with 198–203°C melting point.

General procedure for preparation of olefin 10a and 10b⁴⁸

To an emulsion of 0.040 mol of **8** in THF, 0.040 mol of *n*-BuLi in THF (stock solution 2.5 M) was added under nitrogen. Immediately after addition, the reaction mixture became red. After 2 h under magnetic stirring, 0.040 mol of aldehyde **9** was added. The reaction mixture was stirred for 1 h at room temperature and then allowed to stand overnight. The pale yellow solid was separated by filtration.

The organic layer was washed with cold water, dried over anhydrous MgSO_4 , filtered and the solvent evaporated. The yellow product was distilled under vacuum (**10a**: 130°C/2 mmHg, **10b**: 130°C/3 mmHg) and the fractions containing the products were purified by column chromatography on silica gel using CH_2Cl_2 and C_6H_{14} (2:1) as eluent. A mixture of isomers *Z* and *E* was obtained (**10a**: 59%, **10b**: 47%).

10a: LRMS m/z (% intensity) 176 (M^+ ; 94.3), 161 ($\text{M}^+ - 15$; 100), 145 ($\text{M}^+ - \text{CH}_2\text{CH}_3$; 53.3), 131 ($\text{CH}_3\text{OPh}-\text{C}\equiv\text{C}$; 20.1), 121 ($\text{CH}_3\text{OPhCH}_2$; 38.6), $^1\text{H NMR } \delta$ (ppm) 7.15 (m, 4H); 6.16 (s, 1H); 3.73 (s, 3H); 2.12 (m, 2H); 1.79 (s, 3H); 1.05 (m, 3H).

10b: LRMS m/z (% intensity) 276 (M^+ ; 21), 219 ($\text{M}^+ - 57$; 100); 163 ($219 - (\text{C}(\text{CH}_3)_2\text{H}_5$; 34), 145 ($\text{M}^+ - \text{OSi}(\text{Me})_2t\text{-Bu}$; 3), $^1\text{H NMR } \delta$ (ppm) 6.9 (m, 4H); 6.2 (s, 2H); 2.19 (m, 2H), 1.86 (s, 3H); 1.85 (s, 3H), 1.12 (m, 3H), 0.94 (s, 9H); 0.21 (s, 6H).

General procedure for preparation of olefins **13a** and **13b**⁴⁹

To 0.15 mol of Mg and 1 mL of bromoethane, 0.05 mol of **12** in 10 mL anhydrous THF was added dropwise under heating and stirring. The mixture was refluxed for 2 h. The excess of Mg was rapidly filtered through glass wool under nitrogen and 0.05 mol of dimethylallylbromide in 10 mL THF was added at 0°C. The solution was allowed to warm to room temperature, refluxed for 3 h and cooled to room temperature again. The precipitation of white needle was observed. The solution was poured into 20 mL of cold water and extracted with ethyl acetate (2×50 mL). The extracts were dried over MgSO_4 and concentrated (60°C/30 mmHg). The yellow oil was distilled under vacuum (**13a**: 125°C/3 mmHg, **13b**: 130°C/3 mmHg). Chromatography on silica gel with hexane/methylene chloride (20:1 for **13a** and 1:1 for **13b**) as eluent was performed for further purification (**13a**: 52%, **13b**: 38%).

13a: LRMS m/z (% intensity) 176 (M^+ , 100), 161 ($\text{M}^+ - 15$, 93.2), 147 ($\text{OPhCH}_2\text{CHCH}(\text{CH}_3)$, 10.3), 131 ($\text{PhCH}_2\text{CHCH}(\text{CH}_3)$, 9.9), 121 (MeOPhCH_2 , 22.4), 107 (MeOPh , 8.14), 91 (C_7H_7 , 53.1), 77 (C_6H_5 , 22.4), $^1\text{H NMR } \delta$ (ppm) 6.99–6.46 (m, 4H); 5.12–5.04 (m, 1H); 3.54 (s, 3H); 3.07 (d, 2H, $J=7.35$ Hz); 1.50 (s, 3H); 1.47 (s, 3H), $^{13}\text{C NMR } \delta$ (ppm): 17.19, 25.73, 132.62, 122.97, 34.35, 143.47, 114.10, 159.65, 110.86, 129.26, 120.72, 55.08.

13b: LRMS m/z (% intensity) 276 ($\text{M}^+ - t\text{-Bu}$; 96.4), 219 ($\text{M}^+ - t\text{-Bu}$; 84.9), 204 ($\text{M}^+ - t\text{-Bu}(\text{Me})$; 30.9), 161 ($\text{M}^+ - t\text{-Bu}(\text{Me})_2$; 84.7), $^1\text{H NMR } \delta$ (ppm) 6.96–6.43 (m, 4H); 5.13–5.12 (m, 1H); 3.09 (d, 2H, $J=7.5$ Hz); 1.56 (s, 3H); 1.52 (s, 3H); 0.82 (s, 9H); 0.06 (s, 6H), $^{13}\text{C NMR } \delta$ (ppm) 17.9, 25.7, 132.4, 123.1, 34.2, 143.3, 120.1, 155.6, 117.2, 129.1, 121.3, -4.4, 18.2, 25.8.

General procedure for preparation of bromohydroperoxides **11** and **14**^{2,50}

Anhydrous H_2O_2 in ether. 20 mL of 60% aqueous H_2O_2 were extracted with ether (3×15 mL). The ether phase was

dried over MgSO_4 at 4°C during about 24 h. The peroxide concentration, as determined spectrophotometrically,⁵¹ gives a concentration of the H_2O_2 solution close to 8 M.

Preparation of bromohydroperoxides. To a cooled solution (-20°C) of 0.02 mol of olefin was added 50 mL of an ether H_2O_2 solution ($[\text{H}_2\text{O}_2] \approx 8$ M, 0.4 mol). The mixture was cooled to -40°C and 0.01 mol of 1,3-dibromo-5,5-dimethylhydantoin (DBH) was added in small portions. The initially clear mixture became turbid at each addition of DBH and after some time under stirring became clear again, indicating that DBH has reacted and a new addition can be performed. The total reaction occurs in approximately 1.5 h. The mixture was then allowed to reach 0°C under stirring. The workup of the reaction was performed by washing the cold mixture with cold saturated solutions of Na_2CO_3 (2×30 mL), NaHCO_3 (2×30 mL), $(\text{NH}_4)_2\text{SO}_4$ (2×30 mL) and water (1×30 mL), respectively. The ether layer was dried over MgSO_4 during 1 h at 4°C. The solvent was evaporated at 0°C (30 mmHg) on a rotary evaporator. Due to its instability the product was not purified (row material: **11a**: 77%, **11b**: 67%, **14a**: 69%, **14b**: 80%).

In the case of **14b** a small portion was reserved for chromatographic purification on a silica gel column at -30°C using dichloromethane/hexane (5:1) as eluent. The decomposition of the product was clearly observed during the purification process (just 13% of the row product was obtained as pure product).

14b: $^1\text{H NMR } \delta$ (ppm) 7.81 (s, 1H); 7.20–6.53 (m, 4H); 4.23 (dd, 1H); 3.23–3.14 (m, 1H); 2.62–2.49 (m, 1H); 1.29 (s, 3H); 1.27 (s, 3H); 0.78 (s, 9H); 0.00 (s, 6H).

General procedure for preparation of dioxetanes **I** to **IV**^{2,50}

In a three necked round bottomed flask, equipped with a reflux condenser and an addition funnel, containing 0.0015 mol of β -bromohydroperoxide (**11** or **14**) in 15 mL CH_2Cl_2 and 18-crown-6 (ca. 50 mg), 38 mL of a 2 M KOH solution (0.76 mol) were added dropwise under stirring at 0°C, in the dark. After addition the mixture became pale yellow. The progress of the reaction was monitored by thin layer chromatography on silica gel using $\text{CH}_2\text{Cl}_2/\text{C}_6\text{H}_{14}$ (2:1). After about 1.5 h TLC analysis indicated the total consumption of the corresponding β -bromohydroperoxide. In the case of **III** and **IV** another peroxidic compound, with a R_f similar to that of the β -bromohydroperoxide, was formed as the major product. The mixture was washed with cold solutions of NaCl (2×20 mL) and water (2×10 mL). The organic layer was dried over MgSO_4 during 10 min at 0°C, filtered and the solvent evaporated on a rotary evaporator at 0°C. The purification was performed on a silica gel column at -30°C using a mixture of CH_2Cl_2 and C_6H_{14} as eluent: 2:1, 1:1, 5:1 and 2:1 for **I**, **II**, **III** and **IV**, respectively (**I**: 28%, **II**: 19%, **III**: 3.5%, **IV**: 0.30%).

I: $^1\text{H NMR } \delta$ (ppm) *Z isomer*: 7.68–7.08 (m, 4H); 6.38 (s, 1H); 4.05 (s, 3H); 2.01–1.93 (m, 1H); 1.71–1.67 (m, 1H); 1.94 (s, 3H); 0.85 (t, 3H, $J=7.5$ Hz), *E isomer*: 7.68–7.08 (m, 4H); 6.33 (s, 1H); 4.05 (s, 3H); 2.36–2.28 (m, 2H);

1.36 (s, 3H); 1.28 (t, 3H, $J=7.5$ Hz). ^{13}C NMR δ (ppm): *Z isomer*: 6.29, 28.09, 24.41, 90.93, 91.52, 138.11, 114.23, 159.61, 111.18, 129.60, 118.13, 55.44, *E isomer*: 7.39, 33.78, 20.18, 91.25, 89.81, 137.43, 114.08, 159.52, 111.14, 129.47, 118.00, 55.27.

II: ^1H NMR δ (ppm) *Z isomer*: 7.66–7.40 (m, 4H); 6.10 (s, 1H); 1.72–1.45 (m, 1H); 1.42–1.23 (m, 1H); 1.64 (s, 3H); 0.54 (t, 3H, $J=7.6$ Hz); 0.90 (s, 9H); 0.14 (s, 6H), *E isomer*: 7.66–7.40 (m, 4H); 6.04 (s, 1H); 2.08–1.94 (m, 2H); 1.08 (s, 3H); 0.97 (t, 3H); 0.90 (s, 18H); 0.14 (s, 12H), ^{13}C NMR δ (ppm) *Z isomer*: 6.32, 28.07, 24.41, 91.2, 91.40, 138.0, 118.98, 155.81, 117.88, 129.56, 120.45, –4.48, 19.21, 25.58, *E isomer*: 7.37, 33.78, 20.14, 90.9, 89.72, 137.40, 118.82, 155.81, 117.83, 129.43, 120.32, –4.48, 19.21, 25.58.

III: ^1H NMR δ (ppm) 6.94–6.45 (m, 4H), 5.17–5.03 (m, 1H), 3.52 (s, 3H), 3.05–2.93 (m, 1H), 2.74–2.64 (m, 1H), 1.34 (s, 3H), 1.29 (s, 3H).

IV: ^1H NMR δ (ppm) 7.09–6.48 (m, 4H); 5.26–5.19 (m, 1H); 3.11–3.19 (m, 1H); 2.81–2.71 (m, 1H); 1.42 (s, 3H); 1.18 (s, 3H); 0.77 (s, 9H); 0.01 (s, 6H). ^{13}C NMR δ (ppm) 21.8; 27.7; 87.4; 90.6; 36.8; 136.7; 120.7; 155.6; 118.5; 129.5; 121.8; –4.5; 18.1; 25.5

Preparation of (3-*t*-butyldimethylsilyloxyphenyl)acetaldehyde (15).⁵² The alcohol precursor of this aldehyde was prepared by reacting 3-*t*-butyldimethylsilyloxyphenylbromobenzene with ethylene oxide according to Grignard procedure.⁵³ The alcohol was oxidized with pyridinium chloro chromate (PCC) at room temperature in CH_2Cl_2 for 2 h. The black granular oil formed was washed with ethyl ether (3 \times 50 mL). The organic layer was filtered in a silica gel column and the solvent evaporated. The dark oil obtained was purified by silica gel chromatography, using as eluent hexane/ethyl ether 6:1 (0.65 g—27%).

LRMS—*m/z* (% intensity) 250 (M+; 17), 193 (M+–*t*-Bu; 83), 175 (M+–*t*-Bu –18; 44); 149 (175–(CH_2)₂; 24), 91 (C₇H₇; 22). ^1H NMR δ (ppm) 9.64 (t, 1H, $J=2$, 4 Hz); 7.19–6.63 (m, 4H); 3.55 (d, 2H, $J=2.6$ Hz); 0.92 (s, 9H); 0.11 (s, 6H).

Kinetics studies

Chemiluminescence measurements were performed on a spectrometer SPEX-Fluorolog 1681 with the photomultiplier at 950 V and bandpass set on 27 nm for **I**, **II** and **III** and 20 nm for **IV** and the lamp off. The dioxetane concentrations of the stock solutions were determined spectrophotometrically using the same methodology as used for H_2O_2 : To a cuvette containing 3 mL of a 0.05 M solution of potassium iodide in acetic acid/acetate buffer (pH=3.8, $\mu=0.01$) were added 10 μL of a solution 1.0×10^{-5} M of HRP (horseradish peroxidase) and 10 μL of the dioxetane solution (diluted in CH_3OH). The peroxidic concentration was calculated by measuring the absorbance (*A*) at 353 nm, considering the molar absorptivity coefficient (ϵ) as $2.55\times 10^4 \text{ M}^{-1} \text{ cm}^{-1}$.⁵¹ The toluene used for the unimolecular decomposition experiments was distilled over CaCl_2 , allowed to stand overnight over EDTA, filtered and distilled

again. Anhydrous 99.9% THF and tetrabutylammonium fluoride (1.0 M solution in THF), both from Aldrich Chemical Co., used for the studies of the catalyzed decomposition were handled under nitrogen without further purification. The values calculated for the first and pseudo first order decay constant (*k*) and for the initial chemiluminescence intensity (*I*₀) correspond to the average of at least three measurements and the errors attributed to them are the standard deviation. The calibration of the light intensity was performed by using the luminol standard.³⁷ The kinetics were analyzed using the software MICROCAL v. 6.0, fitting semi-logarithmic plots of Light Emission Intensity vs. time.

Unimolecular decomposition of I to IV

Activation parameters.³⁵ A fluorescence cuvette, containing 3 mL of toluene was brought to the desired temperature, 10–20 μL of the dioxetane stock solution were added rapidly and the kinetics monitored during ~ 3 half-lives. In the case of **I** and **II**, no sensitizer was used and the decay was monitored at 412 nm. For **III** and **IV** the experiments were performed in the presence of DPA (1.0×10^{-2} M) in toluene and the emission monitored at 438 nm. Measurements were recorded at 60 to 85°C, using **[I]**=(6.7 ± 0.8) $\times 10^{-5}$ M, **[II]**=(1.0 ± 0.2) $\times 10^{-4}$ M, **[III]**=(8.3 ± 0.3) $\times 10^{-5}$ M and **[IV]**=(2.1 ± 0.4) $\times 10^{-5}$ M.

Quantum yields.³⁶ The dioxetane stock solution (10–20 μL in toluene) was added to a cuvette, containing 3 mL of the sensitizer solution in toluene pre-heated to 80°C, and the kinetic profiles were recorded using **[I]**=(6.0 ± 0.7) $\times 10^{-6}$ M, **[II]**=(4.7 ± 1.0) $\times 10^{-5}$ M, **[III]**=(8.3 ± 0.3) $\times 10^{-5}$ M, **[IV]**=(2.1 ± 0.4) $\times 10^{-5}$ M, **[DBA]** and **[DPA]**: 1.7×10^{-3} – 1.0×10^{-2} M.

Rate constants (*k*_{obs}): **I**: (2.94 ± 0.18) $\times 10^{-3} \text{ s}^{-1}$, **II**: (3.16 ± 0.12) $\times 10^{-3} \text{ s}^{-1}$, **III**: (3.60 ± 0.13) $\times 10^{-3} \text{ s}^{-1}$, **IV**: (4.28 ± 0.60) $\times 10^{-3} \text{ s}^{-1}$.

Fluoride initiated decomposition of II and IV

The emission spectra from the initiated dioxetane decomposition were obtained by adding 100 μL of a 1.0 M TBAF solution to a cuvette containing dioxetane in 3 mL of THF. The experiments were performed at 25°C for **II** and 7.5°C for **IV**, using **[F⁻]**= 3.2×10^{-2} M, **[II]**=(2.0 ± 0.4) $\times 10^{-5}$ M and **[IV]**=(4.2 ± 0.8) $\times 10^{-5}$ M).

The kinetic experiments were performed with the grating set at the mirror position by treating **II** and **IV** with TBAF (1.0 M solution in THF) in anhydrous THF. All glassware was carefully dried, THF and TBAF solution were handled under nitrogen and the experiment was performed in a cuvette closed with a rubber septum to avoid humidity in the system. As the decomposition kinetics is very fast, the addition of TBAF solution was done very quickly in a dark room.

Fluoride concentration dependence. To a 3 mL cuvette, containing dioxetane in anhydrous THF at 25°C, TBAF was added and the kinetic profiles were measured at different fluoride concentrations, using **[II]**=(2.0 ± 0.4) $\times 10^{-5}$ M,

[IV] = $(4.1 \pm 0.8) \times 10^{-5}$ M and [F] = 6.6×10^{-5} to 6.2×10^{-2} M.

Activation parameters for the initiated decomposition.

These experiments were performed as those for the unimolecular decomposition. The dioxetane was added to a cuvette, containing 3 mL THF at the desired temperature, followed by addition of 100 μ L of TBAF (1.0 M solution in THF) and the kinetic profiles measured, using [III] = $(2.0 \pm 0.4) \times 10^{-5}$ M, [IV] = $(4.1 \pm 0.8) \times 10^{-5}$ M, [F] = 3.2×10^{-2} M, at 0–25°C.

Fluorescent quantum yields.

The fluorescence quantum yields of the cleavage products of II and IV were determined by deprotection of the corresponding silylated aldehydes 9b and 15 by TBAF ([TBAF] = 3.2×10^{-2} M), in THF, using fluorescein as standard (Φ_{FL} = 0.91 in aqueous 0.1 M NaOH).³⁹ The fluorescence spectra of both solutions, fluorescein and the deprotected cleavage products, were measured by exciting the samples at 430 nm under identical experimental conditions.

Chemiluminescence and singlet quantum yields.

In a 3 mL cuvette, containing anhydrous THF and the dioxetane, 100 μ L of the fluoride solution (TBAF 1.0 M solution in THF) were added at 25°C. The kinetic profiles for the decomposition were measured and the integral of the curves calculated. The chemiluminescence quantum yield (Φ_{CHL}) corresponds to the total light emission (area under the curve) divided by the number of moles of dioxetane (n) using [III] = $(2.3 \pm 0.5) \times 10^{-5}$ M and [IV] = $(4.3 \pm 0.7) \times 10^{-5}$ M. After calculation of Φ_{CHL} the singlet quantum yields (Φ_s) were determined according to the following equation: $\Phi_s = \Phi_{CHL} / \Phi_{FL}$.

Acknowledgements

We thank FAPESP, FINEP, CAPES, CNPq and DAAD foundations for financial support. Furthermore, a donation of 60% hydrogen peroxide by Solvay Peróxidos do Brasil Ltda Company is gratefully acknowledged.

References

- Wilson, T. *Int. Rev. Sci.: Phys. Chem. Ser. Two* **1976**, *9*, 265–311.
- (a) Kopecky, K. R.; Mumford, C. *Can. J. Chem.* **1969**, *47*, 709–711. (b) Kopecky, K. R.; Mumford, C. *Abstracts, 51st Annual Conference of Chemical Institute of Canada*, Vancouver, BC, 1968, p 41.
- Staudinger, H. *Chem. Ber.* **1925**, *58*, 1075–1079.
- Bechara, H. J. E.; Wilson, T. *J. Org. Chem.* **1980**, *45*, 5261–5268.
- Adam, W.; Cilento, G. *Chemical and Biological Generation of Excited States*, Academic: New York, 1982.
- Wilson, T. *J. Phys. Org. Chem.* **1995**, *8*, 359–363.
- Koo, J.-Y.; Schuster, G. B. *J. Am. Chem. Soc.* **1978**, *100*, 4496–4503.
- Schuster, G. B.; Dixon, B.; Koo, J.-Y.; Schmidt, S. P.; Schmidt, J. P. *Photochem. Photobiol.* **1979**, *30*, 17–26.
- Schuster, G. B. *Acc. Chem. Res.* **1979**, *12*, 366–373.
- Schmidt, S. P.; Schuster, G. B. *J. Am. Chem. Soc.* **1980**, *102*, 306–314.
- McCapra, F.; Beheshti, I.; Burford, A.; Hann, R. A.; Zaklika, K. A. *J. Chem. Soc., Chem. Commun.* **1977**, 944–946.
- Lee, S.; Singer, L. A. *J. Am. Chem. Soc.* **1980**, *102*, 3823–3829.
- Zakika, K. A.; Kissel, T.; Thayer, A. L.; Burns, P. A.; Schaap, A. P. *Photochem. Photobiol.* **1979**, *30*, 35–44.
- Schaap, A. P.; Gagnon, S. D. *J. Am. Chem. Soc.* **1982**, *104*, 3504–3506.
- Nakamura, K.; Goto, T. *Photochem. Photobiol.* **1979**, *30*, 27–33.
- White, E. H.; Wörther, H.; Seliger, H. H.; McElroy, W. D. *J. Am. Chem. Soc.* **1966**, *88*, 2015–2019.
- Schaap, A. P.; Chen, T.-S.; Handley, R. S.; De Silva, R.; Giri, B. P. *Tetrahedron Lett.* **1987**, *28*, 1155–1158.
- Schaap, A. P.; Handley, R. S.; Giri, B. P. *Tetrahedron Lett.* **1987**, *28*, 935–938.
- Schaap, A. P.; Sandison, M. D.; Handley, R. S. *Tetrahedron Lett.* **1987**, *28*, 1159–1162.
- Bronstein, I.; Voyta, J. C.; Lazzari, K. G.; Murphy, O.; Edwards, B.; Kricka, L. J. *Biotechniques* **1992**, *12*, 748–753.
- Nishizono, I.; Iida, S.; Suzuki, N.; Kawada, H.; Murakami, H.; Ashihara, Y.; Okada, M. *Clin. Chem.* **1991**, *37*, 1639–1644.
- Lim, T.; Komoda, Y.; Nakamura, N.; Matsunaga, T. *Anal. Chem.* **1999**, *71*, 1298–1302.
- Beck, S.; Köster, H. *Anal. Chem.* **1990**, *62*, 2258–2270.
- Adam, W.; Reinhardt, D.; Sahamoller, C. R. *Analyst* **1996**, *121*, 1527–1531.
- Matsumoto, M.; Watanabe, N.; Kobayashi, H.; Azami, M.; Ikawa, H. *Tetrahedron Lett.* **1997**, *38*, 411–414.
- Matsumoto, M.; Ishihara, T.; Watanabe, N.; Hiroshima, T. *Tetrahedron Lett.* **1999**, *40*, 4571–4574.
- Watanabe, N.; Sugauma, H.; Kobayashi, H.; Mutoh, H.; Katao, Y.; Matsumoto, M. *Tetrahedron* **1999**, *55*, 4287–4298.
- Watanabe, N.; Kobayashi, H.; Azami, M.; Matsumoto, M. *Tetrahedron* **1999**, *55*, 6831–6840.
- Adam, W.; Reinhardt, D. *Liebigs Ann.* **1997**, 1359–1364.
- Imanishi, T.; Ueda, Y.; Tainaka, R.; Miyashita, K. *Tetrahedron Lett.* **1997**, *38*, 841–844.
- Adam, W.; Bronstein, I.; Trofimov, A. V.; Vasil'ev, R. F. *J. Am. Chem. Soc.* **1999**, *121*, 958–961.
- Nery, A. L. P.; Röpke, S.; Catalani, L. H.; Baader, W. J. *Tetrahedron Lett.* **1999**, *40*, 2443–2446.
- Adam, W.; Baader, W. J. *J. Am. Chem. Soc.* **1985**, *107*, 410–416.
- Murov, S. L.; Carmichael, I.; Hug, G. L. *Handbook of Photochemistry*, Marcel Dekker: New York, 1993.
- Adam, W.; Zinner, K. *Chemical and Biological Generation of Excited States*, Academic: New York, 1982 (p 153–189).
- Adam, W. *Chemical and Biological Generation of Excited States*, Academic: New York, 1982 (p 115–152).
- Lee, J.; Wesley, A. S.; Fregson III, J. F.; Seliger, H. H. *Bio-luminescence in Progress*, Princeton University Press: Princeton, 1966 (p 35–43).
- Lee, J.; Seliger, H. H. *Photochem. Photobiol.* **1972**, *15*, 227–237.
- Miller, J. N. *Standards in Fluorescence Spectroscopy*, Chapman and Hall: New York, 1981; vol. 2.
- Baumstark, A. L.; Dunams, T.; Roskamp, P. C.; Wilson, C. E. *J. Org. Chem.* **1983**, *48*, 261–263.
- Baumstark, A. L.; Retter, C. A.; Tehrani, K.; Kellog, C. J. *Org. Chem.* **1987**, *52*, 3308–3311.

42. Closs, G. L.; Calcaterra, L. T.; Green, N. J.; Penfield, K. W.; Miller, J. R. *J. Phys. Chem.* **1986**, *90*, 3673–3683.
43. Catalani, L. H.; Wilson, T. *J. Am. Chem. Soc.* **1989**, *111*, 2633–2639.
44. Zimmerman, H. E.; Somasekhara, S. *J. Am. Chem. Soc.* **1963**, *85*, 922–927.
45. Pincock, J. A.; Wedge, P. J. *J. Org. Chem.* **1994**, *59*, 5578–5587.
46. Fleming, S. A.; Jensen, A. W. *J. Org. Chem.* **1996**, *61*, 7040–7044.
47. Perrin, D. D.; Armarego, W. L. F. *Purification of Laboratory Chemicals*, Reed Educational and Professional Ltd: Oxford, 1996.
48. Wittig, G.; Schoellkopf, U. *Org. Synth.* **1960**, *40*, 66–68.
49. Lajis, N. Hj.; Khan, M. N. *Tetrahedron* **1992**, *48*, 1109–1114.
50. Baumstark, A. L. *Singlet Oxygen*, CRC: Baton Rouge, LA, 1985; Vol. II.
51. Cotton, M. L.; Dunford, H. B. *Can. J. Chem.* **1973**, *51*, 582–587.
52. Corey, E. J.; Suggs, J. W. *Tetrahedron Lett.* **1975**, *31*, 2647–2650.
53. Lai, Y.-H. *Synthesis* **1981**, 585–604.